The 2009 IEEE/RSJ International Conference on
Intelligent Robots and Systems
October 11-15, 2009 St. Louis, USA

Efficiency Analysis of 2-period Dynamic Bipdal Gaits

Fumihiko Asano

Abstract— **This paper investigates the efficiency of a 2-period gait from the kinetic energy view-point. First, we formulate a steady 2-period gait for a compass-like bipedal robot by using a simple recurrence formula for the kinetic energy of an asymmetric rimless wheel. Second, we theoretically show that, in the case that the mean value of the hip angle is constant, the generated 2-period steady gait is less efficient than a 1-period symmetric one in terms of kinetic energy. We also show that the symmetric gait is not always optimal from another viewpoint. We then investigate the validity of the derived method through numerical simulations of virtual passive dynamic walking. Other approaches, delayed feedback control and a quasi-constraint on the impact posture, are also considered for stabilization to a 1-period gait and their effects are discussed.**

I. Introduction

Limit cycle walkers based on the robot's own passive dynamics are good examples of efficient bipedal locomotion. Since McGeer's passive dynamic walking (PDW) [1], many follow-on studies have been undertaken all over the world. One of the major interests is achieving efficient level dynamic walking with small actuators. The authors have proposed several methods for generating efficient bipedal gaits. Among them, virtual passive dynamic walking (VPDW) [2] and parametrically excited walking [3] are the major examples.

Studies on PDW as a nonlinear hybrid dynamical system have also been conducted. Nonlinear phenomena in PDW are very complicated, and their investigation has proceeded with difficulty for the last decade. The most interesting phenomenon that passive-dynamic walkers exhibit is the period-doubling bifurcation and chaotic behavior discovered by Goswami *et al.* They discovered a period-doubling bifurcation in a passive gait on a gentle slope and numerically showed that a compass-like biped robot exhibits period-doubling bifurcation by changing the walking system's parameters such as slope and leg-mass location [4]. After that, Garcia *et al.* showed that the simplest walking model and kneed model also exhibit period-doubling bifurcation [5][6][7]. Goswami *et al.* [8] and Sano *et al.* [9] investigated the bifurcation mechanism by using the eigenvalues of the Poincaré return map. Osuka and Kirihara experimentally confirmed the phenomenon [10]. In addition, controlling chaos in dynamic gaits has been investigated. The OGY method [11] and delayed feedback control (DFC) [12] are the major approaches to controlling or stabilizing chaos. These have been used for stabilizing a multiple period gait into a 1-period one. Sugimoto and Osuka used DFC to stabilize a passive-dynamic gait and generated an unstable 1-period gait [13]. Suzuki and Furuta also used the OGY method for the stabilization [14].

As manifested by the above studies, the period-doubling bifurcation phenomenon and the properties of multiple-period gaits in PDW have been widely studied. However, the reason why this phenomenon emerges has not yet been discovered, and the effects that bifurcation might have on gait efficiency are still unclear. Although the application of multiple-period or chaotic behavior to legged locomotion control has been expected, no useful methods have been proposed to date. It is known that the hip-joint damper can eliminate the chaotic behavior and create a 1-period limit cycle. This extends the stable domain and does not have any advantages from an engineering standpoint. Meanwhile, the authors observed that the efficiency of a 2-period gait grows worse rapidly after the first bifurcation point [15] and have shown that the gait efficiency of an asymmetric gait would be low.

In this paper, we investigate the efficiency and optimality of a 2-period gait in terms of the kinetic energy. The convergent kinetic energy is to be an indicator of gait efficiency. A steady 2-period gait is formulated by using recurrence formulas of kinetic energy just before impact of an asymmetric rimless wheel on the walking surface. This formula can specify the steady discrete dynamics of general 2-period limit cycle walking. We then theoretically investigate the relation between the gait efficiency and gait symmetry from a kinetic energy view-point. Furthermore, other approaches to stabilization of 2-period gaits are numerically investigated and their effects are evaluated.

II. Stability Principle of a Rimless Wheel

We first describe the stability mechanism of a rimless wheel. Since the detailed theory was already explained in [16], we only outline it here.

Fig. 1 (a) shows the model of a rimless wheel. Let α [rad] be the angle between the frames, and θ [rad] be the angle with respect to vertical. We assume that the total mass, M [kg], is concentrated at the central point and the leg frames have no mass. We also assume that $0 \leq \alpha \leq \pi$.

Let K^- [J] be the kinetic energy just before impact; it satisfies the following recurrence formula:

$$K^-[i+1] = \varepsilon K^-[i] + \Delta E, \tag{1}$$

where i is the step number, ε [-] is the energy-loss coefficient, and ΔE [J] is the restored mechanical energy. The energy-

F. Asano is with the School of Information Science, Japan Advanced Institute of Science and Technology, Nomi, Ishikawa 923-1292, Japan fasano@jaist.ac.jp

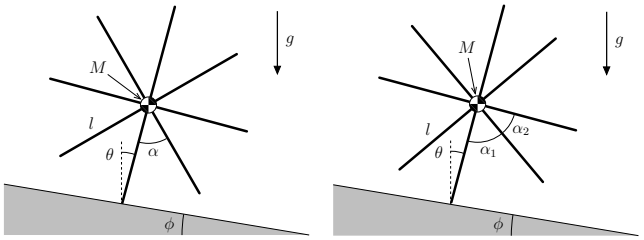

(a) Symmetric model (b) Asymmetric model

Fig. 1. Two rimless wheel models.

loss coefficient is defined as

$$\varepsilon := \frac{K^+}{K^-}, \tag{2}$$

where K^+ [J] is the kinetic energy just after impact. In this rimless wheel model, ε and ΔE are given by the following equations.

$$\varepsilon = \cos^2\alpha, \quad \Delta E = 2Mlg\sin\frac{\alpha}{2}\sin\phi \tag{3}$$

The generated gait becomes asymptotically stable under the assumption that the next heel-strike always occurs, and K^- converges to

$$K^-[\infty] := \lim_{i\to\infty} K^-[i] = \frac{\Delta E}{1-\varepsilon}. \tag{4}$$

Note that ε is convex upward in the range of $0 \le \alpha \le \pi/4$, and ΔE is proportional to the step length. These properties are common to the original PDW [1] and VPDW [2], and they are very important for understanding the gait efficiency.

Since the 2-D rimless wheel model is a very simple way to reproduce the discrete walking behavior, it has often been used for analyzing gait efficiency and robustness. In the following, we utilize it for representing the discrete dynamics of 2-period limit cycle walking.

III. Efficiency of an Asymmetric Rimless Wheel

A. Preliminaries

Fig. 1 (b) shows the model of an asymmetric rimless wheel. Let α_1 and α_2 [rad] be the relative angles between the frames. We assume the following magnitude relation:

$$\alpha_2 \le \alpha \le \alpha_1, \tag{5}$$

where we also define their mean value, α [rad], as

$$\alpha := \frac{\alpha_1+\alpha_2}{2}. \tag{6}$$

Let ε_j be the energy-loss coefficient and ΔE_j be the restored mechanical energy corresponding to the angle α_j, as follows.

$$\varepsilon_j := \varepsilon(\alpha_j) = \cos^2\alpha_j \quad (i=1,2) \tag{7}$$

$$\Delta E_1 = 2Mlg\sin\frac{\alpha}{2}\sin\left(\phi+\frac{\alpha_1-\alpha_2}{4}\right) \tag{8}$$

$$\Delta E_2 = 2Mlg\sin\frac{\alpha}{2}\sin\left(\phi-\frac{\alpha_1-\alpha_2}{4}\right) \tag{9}$$

Here, ΔE_i were derived from the law of conservation of mechanical energy, and are given as changes in potential energy. They satisfy the following magnitude relations.

$$\varepsilon_1 \le \varepsilon \le \varepsilon_2, \quad \Delta E_2 \le \Delta E \le \Delta E_1 \tag{10}$$

Since ε_j is convex upward in the range of $0 \le \alpha_j \le \pi/4$, the following magnitude relation holds:

$$\varepsilon \ge \frac{\varepsilon_1+\varepsilon_2}{2} \ge \sqrt{\varepsilon_1\varepsilon_2}, \tag{11}$$

where the second inequality is an arithmetic and geometric means inequality. The equalities in Eq. (11) hold when $\alpha_1 = \alpha_2$. On the other hand, the mean value of restored mechanical energy can be written as follows:

$$\frac{\Delta E_1+\Delta E_2}{2} = 2Mlg\sin\frac{\alpha}{2}\sin\phi\cos\frac{\alpha_1-\alpha_2}{4}. \tag{12}$$

This leads to the following magnitude relation:

$$\Delta E \ge \frac{\Delta E_1+\Delta E_2}{2}. \tag{13}$$

The equality holds when $\alpha_1 = \alpha_2$.

By using the above variables, we can formulate the discrete dynamics of a rimless wheel. Let K_j^- be the kinetic energy just before an impact corresponding to the hip angle, α_j. The following two recurrence formulas hold.

$$K_2^-[2i+1] = \varepsilon_1 K_1^-[2i] + \Delta E_2 \tag{14}$$

$$K_1^-[2i+2] = \varepsilon_2 K_2^-[2i+1] + \Delta E_1 \tag{15}$$

In the following, we will analyze the gait efficiency of an asymmetric rimless wheel in terms of kinetic energy.

B. Optimality when α is constant

We first investigate the case in which α [rad] is constant. By substituting Eq. (14) into Eq. (15) and eliminating K_2^-, we obtain

$$K_1^-[2i+2] = \varepsilon_1\varepsilon_2 K_1^-[2i] + \varepsilon_2\Delta E_2 + \Delta E_1. \tag{16}$$

This leads to

$$K_1^-[\infty] = \frac{\varepsilon_2\Delta E_2+\Delta E_1}{1-\varepsilon_1\varepsilon_2}. \tag{17}$$

In the same way, we obtain

$$K_2^-[\infty] = \frac{\varepsilon_1\Delta E_1+\Delta E_2}{1-\varepsilon_1\varepsilon_2}. \tag{18}$$

The mean value becomes

$$\begin{aligned} K_m^-[\infty] &:= \frac{1}{2}\left(K_1^-[\infty]+K_2^-[\infty]\right) \\ &= \frac{\varepsilon_1\Delta E_1+\varepsilon_2\Delta E_2+\Delta E_1+\Delta E_2}{2(1-\varepsilon_1\varepsilon_2)}. \end{aligned} \tag{19}$$

Define the mean values of Eqs. (11) and (13) as

$$\varepsilon_m := \frac{\varepsilon_1+\varepsilon_2}{2}, \ \Delta E_m := \frac{\Delta E_1+\Delta E_2}{2}, \tag{20}$$

and consider the following magnitude relation:

$$\begin{aligned} \varepsilon_m\Delta E_m - \frac{\varepsilon_1\Delta E_1+\varepsilon_2\Delta E_2}{2} &= \frac{(\varepsilon_2-\varepsilon_1)(\Delta E_1-\Delta E_2)}{4} \\ &\ge 0, \end{aligned} \tag{21}$$

and the relation of arithmetic and geometric means of Eq. (11):

$$\varepsilon_m \ge \sqrt{\varepsilon_1\varepsilon_2}. \tag{22}$$

The upper limit of Eq. (19) can then be derived as

$$\begin{aligned} K_m^-[\infty] &\le \frac{\varepsilon_m\Delta E_m+\Delta E_m}{1-\varepsilon_m^2} = \frac{(1+\varepsilon_m)\Delta E_m}{(1+\varepsilon_m)(1-\varepsilon_m)} \\ &= \frac{\Delta E_m}{1-\varepsilon_m}. \end{aligned} \tag{23}$$

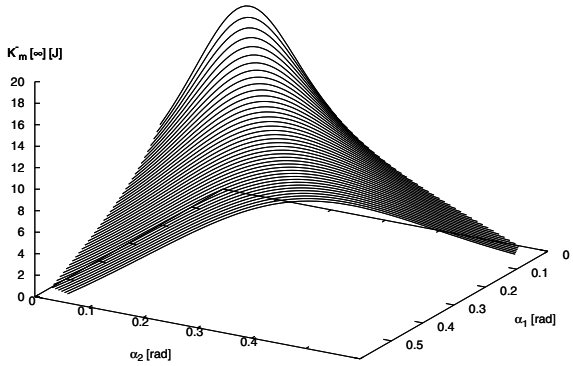

Fig. 2. 3D plot of $K_m^-[\infty]$ with respect to α_1 and α_2. Each curve keeps α constant.

This is the upper limit of $K_m^-[\infty]$ common to general 2-period gaits.

By using the two magnitude relations of Eqs. (11) and (13), the magnitude relation for $K^-[\infty]$ can be derived as follows.

$$K_m^-[\infty] \leq \frac{\Delta E_m}{1-\varepsilon_m} \leq \frac{\Delta E}{1-\varepsilon} = K^-[\infty] \tag{24}$$

The equality holds when $\Delta E = \Delta E_m$ and $\varepsilon = \varepsilon_m$, and this is equivalent to $\alpha_1 = \alpha_2 = \alpha$.

Fig. 2 shows the 3D plot of $K_m^-[\infty]$ with respect to α_1 and α_2 where $M = 20.0$ [kg] and $l = 1.0$ [m]. The 3D plot was drawn with convex curves. Each curve corresponds to a given constant α ($0.10 \leq \alpha \leq 0.30$). We can see that the optimal solution is $\alpha_1 = \alpha_2 (= \alpha)$ on each curve.

As $\alpha_1 \to 2\alpha$ and $\alpha_2 \to 0$, the generated gait becomes a symmetric 1-period gait whose recurrence formula is

$$K_1^-[i+1] = \varepsilon_1 K_1^-[i] + \Delta E_1, \tag{25}$$

where $\varepsilon_1 = \cos^2(2\alpha)$ and $\Delta E_1 = 2Mlg \sin\alpha \sin\phi$. In this case, the convergent kinetic energy becomes the lowest.

Based on the above discussion, we can conclude that gait efficiency grows worse as the gait changes into a 2-period one because the step grows larger or the energy-loss coefficient becomes smaller.

The magnitude relation (Eq. (13)) holds for a dynamic bipedal gait such as PDW [1] or VPDW [2]. The relation for the energy-loss coefficient, however, does not always hold because it is affected by the angular velocities just before impact. Except for the gait with a constraint on the impact posture [16], the condition of Eq. (11) cannot be guaranteed.

C. Optimality when α_1 is constant

Fig. 3 plots the contour of the 3D plot in Fig. 2 in the α_1-α_2 plane. We can see that the contour is symmetric with $\alpha_1 = \alpha_2$. Note that the optimal solution, $\alpha_1 = \alpha_2$, is obtained in the case that the mean value, α, is constant (See direction A in Fig. 3).

In the case that α_1 is fixed, the optimal solution does not become $\alpha_1 = \alpha_2$, as one can see from direction B in Fig. 3. It is not easy to find the solution of α_2 for $F(\alpha_2) = 0$ analytically.

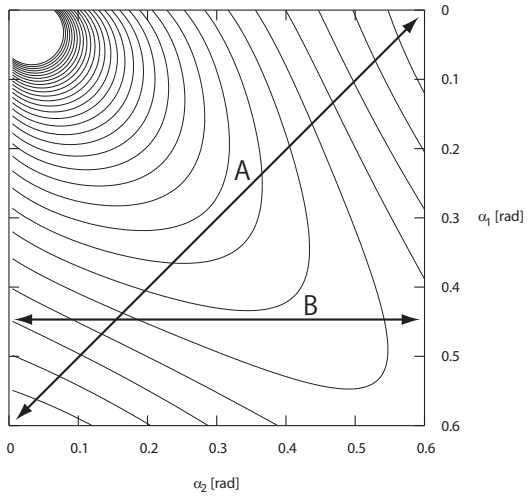

Fig. 3. Contour of $K_m^-[\infty]$ with respect to α_1 and α_2.

IV. Virtual Passive Dynamic Walking

This section investigates the validity of the analysis in the previous section through numerical simulations of VPDW.

A. Biped robot model

Fig. 4 shows a planar fully actuated biped model. Since the model is the same as those of [2][16], we only outline it. This model consists of 2-link and 3-point masses and has feet whose mass and thickness can be neglected. Let $\boldsymbol{\theta} = \begin{bmatrix}\theta_1 & \theta_2\end{bmatrix}^{\mathrm{T}}$ be the generalized coordinate vector; the robot's dynamic equation is

$$\boldsymbol{M}(\boldsymbol{\theta})\ddot{\boldsymbol{\theta}} + \boldsymbol{h}(\boldsymbol{\theta}, \dot{\boldsymbol{\theta}}) = \boldsymbol{S}\boldsymbol{u} = \begin{bmatrix}1 & 1\\ 0 & -1\end{bmatrix}\begin{bmatrix}u_1\\ u_2\end{bmatrix}, \tag{26}$$

where u_1 and u_2 are the ankle and hip joint torques. We assume that the heel strike is inelastic and the stance and swing legs are exchanged instantaneously.

B. Controller synthesis and typical 2-period gait

As the most basic approach to achieve the two magnitude relations of Eq. (11) and (13), we can consider VPDW with a constraint on the impact posture, which is termed as the constrained compass-gait [16]. In VPDW, the joint torques are determined to satisfy the following relation between the X-position of CoM, X_g, and the total mechanical energy:

$$\frac{\partial E}{\partial X_g} = Mg\tan\phi, \tag{27}$$

where ϕ [rad] is the virtual slope angle and $M := m_H + 2m$ [kg] is the robot's total mass. Eq. (27) can be transformed into

$$\dot{E} = \dot{\theta}_1 u_1 + \dot{\theta}_H u_2 = Mg\tan\phi \dot{X}_g, \tag{28}$$

and we determine u_1 and u_2 according to the priority order. Hence, we will realize VPDW with a constraint on the impact posture.

We first synthesize the motion controller for generating ΔE_2 in Eq. (14). During the stance phase, the hip angle θ_H must move smoothly during the change from $-2\alpha_1$ to $2\alpha_2$.

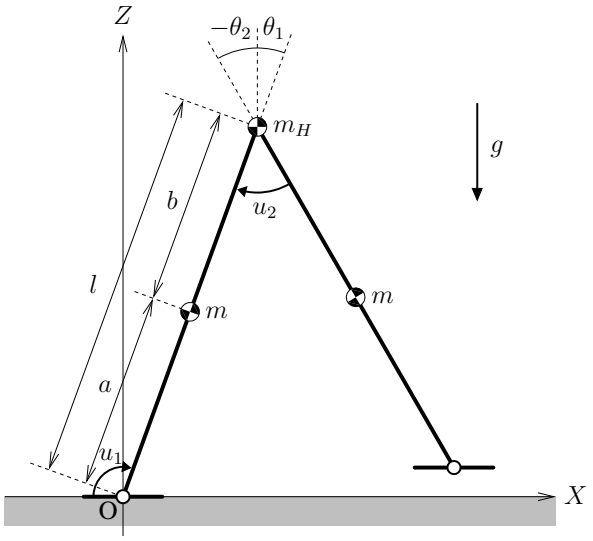

Fig. 4. Model of planar fully actuated compass-like biped robot. This model can exhibit passive dynamic walking on a gentle slope.

TABLE I

PHYSICAL PARAMETERS OF BIPED ROBOT

m_H	10.0	kg
m	5.0	kg
a	0.5	m
b	0.5	m
$l\ (=a+b)$	1.0	m

We introduce the following 5-order desired-time trajectory.

$$\theta_{H\mathrm{d}}(t) = \begin{cases} a_{51}t^5 + a_{41}t^4 + a_{31}t^3 + a_{01} & (0 \le t < T_{\mathrm{set}}) \\ 2\alpha_2 & (t \ge T_{\mathrm{set}}) \end{cases} \tag{29}$$

The coefficients, a_{i1}, are determined so that they satisfy

$$\ddot{\theta}_{H\mathrm{d}}(0) = 0,\ \dot{\theta}_{H\mathrm{d}}(0) = 0,\ \theta_{H\mathrm{d}}(0) = -2\alpha_1,$$
$$\ddot{\theta}_{H\mathrm{d}}(T_{\mathrm{set}}) = 0,\ \dot{\theta}_{H\mathrm{d}}(T_{\mathrm{set}}) = 0,\ \theta_{H\mathrm{d}}(T_{\mathrm{set}}) = 2\alpha_2,$$

and are given by

$$\begin{bmatrix} a_{51} \\ a_{41} \\ a_{31} \end{bmatrix} = \begin{bmatrix} T_{\mathrm{set}}^5 & T_{\mathrm{set}}^4 & T_{\mathrm{set}}^3 \\ 5T_{\mathrm{set}}^4 & 4T_{\mathrm{set}}^3 & 3T_{\mathrm{set}}^2 \\ 20T_{\mathrm{set}}^3 & 12T_{\mathrm{set}}^2 & 6T_{\mathrm{set}} \end{bmatrix}^{-1} \begin{bmatrix} 2\left(\alpha_1 + \alpha_2\right) \\ 0 \\ 0 \end{bmatrix},$$

and $a_{01} = -2\alpha_1$. The coefficients, a_{i2}, of the desired-time trajectory for generating ΔE_1 in Eq. (15) are determined in the same manner. a_{52}, a_{42}, and a_{32} are determined with the same equation and $a_{02} = -2\alpha_2$. The desired settling time, T_{set} [s], is chosen empirically. Let T_1 and T_2 [s] be the steady step periods; we found that a constrained compass-gait could be successfully generated if the settling-time condition, $T_{\mathrm{set}} \le T_1, T_2$, is satisfied.

Next, let us consider the output following control for the desired-time trajectory. We first constrain the impact posture by actuating the hip joint. We resolve the control input vector as

$$\boldsymbol{S}\boldsymbol{u} = \begin{bmatrix} 1 \\ 0 \end{bmatrix} u_1 + \begin{bmatrix} 1 \\ -1 \end{bmatrix} u_2 =: \boldsymbol{S}_1 u_1 + \boldsymbol{S}_2 u_2, \tag{30}$$

and conduct input-output linearization. The hip-joint angle for the control output can be written as $\theta_H = \boldsymbol{S}_2^{\mathrm{T}}\boldsymbol{\theta}$, and its second-order derivative with respect to time becomes

$$\ddot{\theta}_H = \boldsymbol{S}_2^{\mathrm{T}}\ddot{\boldsymbol{\theta}} = \boldsymbol{S}_2^{\mathrm{T}}\boldsymbol{M}(\boldsymbol{\theta})^{-1}\left(\boldsymbol{S}_2 u_2 - \boldsymbol{h}(\boldsymbol{\theta}, \dot{\boldsymbol{\theta}})\right). \tag{31}$$

We will consider the following control input to achieve $\theta_H \to \theta_{H\mathrm{d}}$:

$$u_2 = \left(\boldsymbol{S}_2^{\mathrm{T}}\boldsymbol{M}(\boldsymbol{\theta})^{-1}\boldsymbol{S}_2\right)^{-1}\left(\bar{u} + \boldsymbol{S}_2^{\mathrm{T}}\boldsymbol{M}(\boldsymbol{\theta})^{-1}\boldsymbol{h}(\boldsymbol{\theta}, \dot{\boldsymbol{\theta}})\right), \tag{32}$$

$$\bar{u} = \ddot{\theta}_{H\mathrm{d}} + k_{\mathrm{d}}\left(\dot{\theta}_{H\mathrm{d}} - \dot{\theta}_H\right) + k_{\mathrm{p}}\left(\theta_{H\mathrm{d}} - \theta_H\right), \tag{33}$$

where k_{p} and k_{d} are the PD gains and are positive constants.

The ankle-joint torque u_1 is obtained from u_2 to be

$$u_1 = \frac{Mg\tan\phi\dot{X}_g - \dot{\theta}_H u_2}{\dot{\theta}_1}. \tag{34}$$

We must assume that $\dot{\theta}_1 > 0$ holds during stance phases, and this condition is satisfied in VPDW.

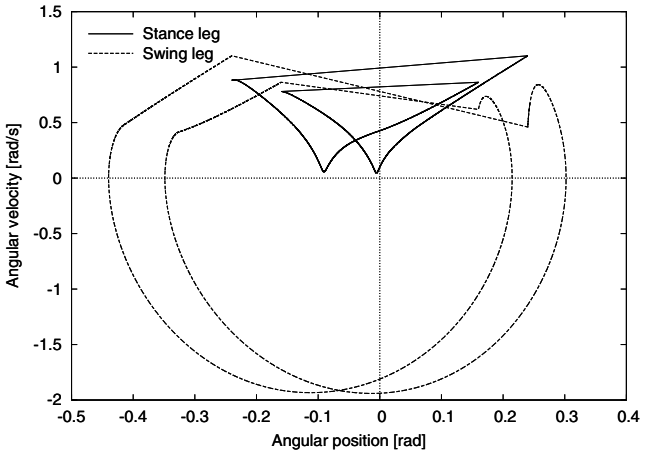

Fig. 5. Phase portrait of steady 2-period constrained compass-gait. Stance and swing leg are plotted independently.

Fig. 5 shows the phase portrait of a steady 2-period constrained compass-gait where $\alpha_1 = 0.24$, $\alpha_2 = 0.16$, and $\phi = 0.02$ [rad]. The PD gains were chosen sufficiently large to achieve trajectory tracking control and a constraint on the impact posture with satisfactory accuracy. The figure shows that we return to the original position after two laps.

C. Restored mechanical energy

In 2-period gaits, the restored mechanical energy is determined not only by the control inputs but also by the difference in the potential energies at impact. Eq. (14) can be detailed as

$$K_2^-[\infty] + P_2[\infty] = \varepsilon_1 K_1^-[\infty] + P_1[\infty] + \int_{0^+}^{T_2^-} \dot{\boldsymbol{\theta}}^{\mathrm{T}}\boldsymbol{S}\boldsymbol{u}\ \mathrm{d}t, \tag{35}$$

where P_1 and P_2 are the potential energies corresponding to each impact. By grouping the terms in Eq. (35) except those of the kinetic energy, ΔE_2 of (14) is can be derived as

$$\begin{aligned} \Delta E_2 &= \int_{0^+}^{T_2^-} \dot{\boldsymbol{\theta}}^{\mathrm{T}}\boldsymbol{S}\boldsymbol{u}\ \mathrm{d}t + P_1[\infty] - P_2[\infty] \\ &= Mgl\tan\phi\left(\sin\alpha_1 + \sin\alpha_2\right) \\ &\quad + \left(m_H l + 2ma\right)g\left(\cos\alpha_1 - \cos\alpha_2\right). \end{aligned} \tag{36}$$

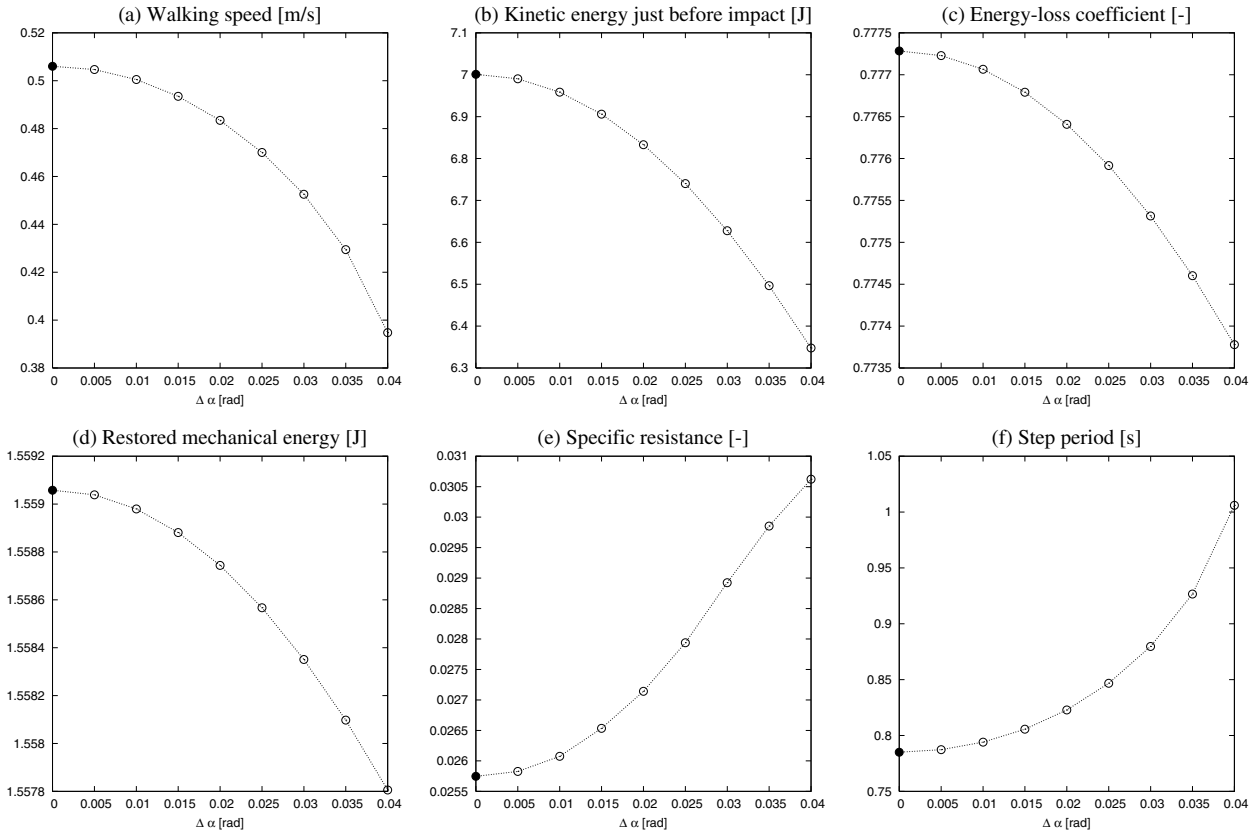

Fig. 6. Gait descriptors of constrained compass-gait where α is constant. Here, (a) is the walking speed, (b) the kinetic energy just before impact, (c) the energy-loss coefficient, (d) the restored mechanical energy, (e) the specific resistance, and (f) the step period.

In the same way, ΔE_1 of Eq. (15) can be derived as

$$\begin{aligned}\Delta E_1 \;=\; & Mgl\tan\phi\,(\sin\alpha_1+\sin\alpha_2)\\ & -(m_H l+2ma)\,g\,(\cos\alpha_1-\cos\alpha_2)\,. \end{aligned}\quad (37)$$

From Eq. (36) and (37), the magnitude relation of Eq. (13) can be written as follows.

$$\begin{aligned}\frac{\Delta E_1+\Delta E_2}{2} \;&=\; 2Mgl\tan\phi\sin\alpha\cos\frac{\alpha_1-\alpha_2}{2}\\ &\le\; 2Mgl\tan\phi\sin\alpha=\Delta E\end{aligned}\quad (38)$$

D. Analysis of gait efficiency

In biped walking systems, unlike in rimless wheels, maximizing K^- is not always equivalent to maximizing the gait efficiency for the following reasons.

- The convergent level of K^- is not always equivalent to that of the walking speed.
- Even if the convergent kinetic energy is at a maximum, energy efficiency is not always maximum because it is evaluated in another way.

1) When α is constant: Fig. 6 shows the analysis results of the constrained compass-gait when α is constant. All indicated data are mean values. $\Delta\alpha := \alpha_1-\alpha=\alpha-\alpha_2\ge 0$ is used for the horizontal axis. We can see that the larger $\Delta\alpha$ is, the more asymmetric the gait becomes. The value at which $\Delta\alpha=0$ (1-period gait, symmetric) is plotted with a solid circle to distinguish it from other 2-period cases.

From Fig. 6 (a) and (b), we can see that the walking speed and kinetic energy monotonically decrease as the gait asymmetry grows. From (c) and (d), we can confirm that the two magnitude relations of Eqs. (11) and (13) hold. (e) and (f) are plotted as references. These results can be explained on the basis of (a) and (b) as follows. If the mean value of the step length is kept constant, the step period should monotonically increase in inverse proportion to the walking speed, which monotonically decreases because of the gait asymmetrization. Since the consumed energy stays nearly constant in this case, the specific resistance should increase as the walking speed decreases.

2) When α_1 is constant: Fig. 7 shows the analysis results where α_1 is constant. The horizontal axis is the mean value of the hip-joint angle, α, except in (f) where α_1 and α_2 are plotted on the horizontal axis and we have indicated the corresponding step periods. From (a) and (b), we can see that the walking speed and kinetic energy increase with decreasing α. In contrast to the above case, the gait efficiency improves as the gait asymmetry grows. (c) shows that ε_m monotonically increases with decreasing α, i.e. with the mean value of the step length, in accordance with the constraint on the impact posture. (d) shows that ΔE_m monotonically decreases with increasing α in accordance with Eq. (38). (e) shows that the specific resistance grows worse because of the gait asymmetrization; however, this change is insignificant compared with the change in Fig. 6 (e). We plotted the step period in (f) to show that the gait is impossible to generate because the step period is too short

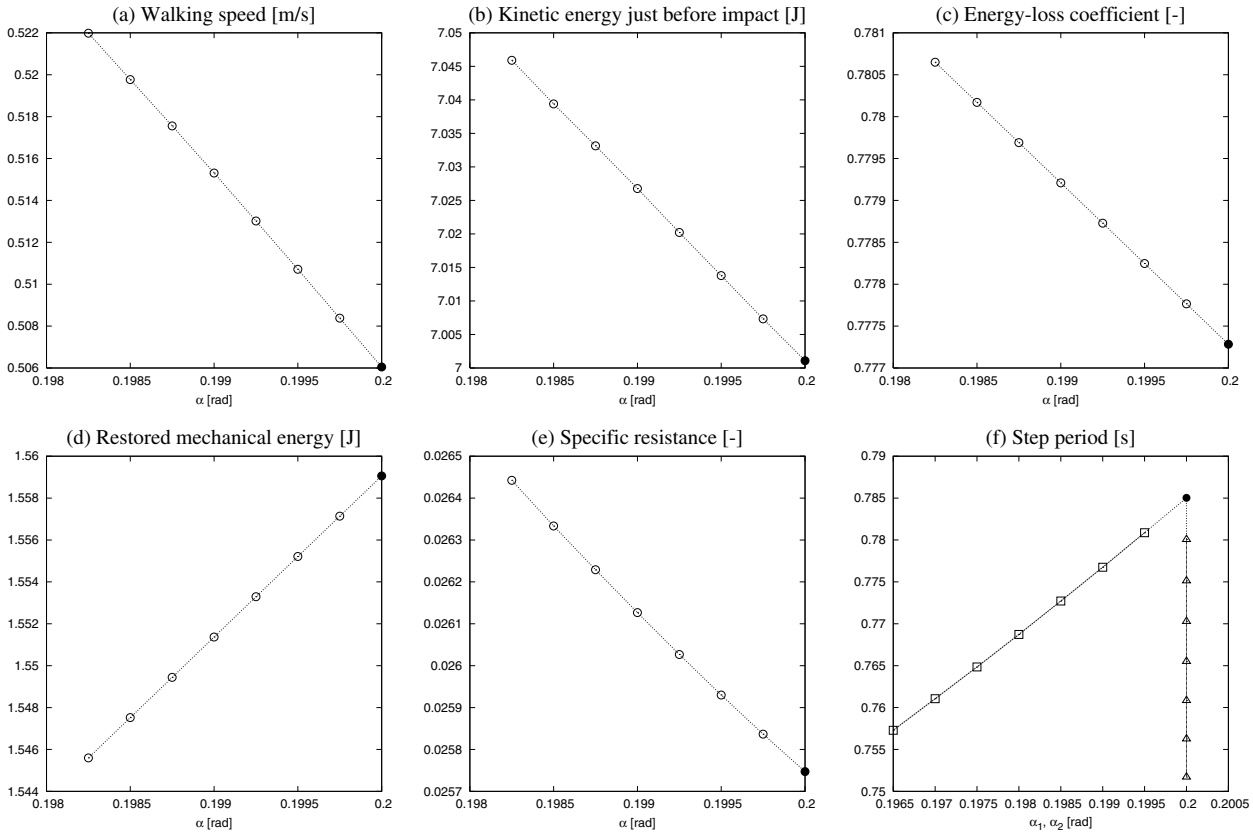

Fig. 7. Gait descriptors of constrained compass-gait where α_1 is constant. Here, (a) is the walking speed, (b) the kinetic energy just before impact, (c) the energy-loss coefficient, (d) the restored mechanical energy, (e) the specific resistance, and (f) the step period.

and thus the settling-time condition cannot be satisfied. The two periods are indicated as "$\triangle$" and "$\square$"; both decrease monotonically and $\triangle$ approaches $T_{\rm set} = 0.75$ [s].

V. Delayed Feedback Control

This section investigates the effect of delayed feedback control (DFC) [12]. Sugimoto and Osuka employed this control law to stabilize a 2-period passive-dynamic gait [13], and we will adopt their approach.

As Goswami *et al.* showed numerically, a PDW robot exhibits a period-doubling bifurcation from about $\phi = 0.076$ [rad]. We will thus consider a 2-period passive compass-gait in which $\phi = 0.080$ [rad] and its stabilization to an unstable 1-period gait. A convergent steady 2-period gait has $\alpha_1 = 0.3248$, $\alpha_2 = 0.3001$ [rad], $\varepsilon_1 = 0.5182$, $\varepsilon_2 = 0.5331$ [-], $\Delta E_1 = 10.745$, $\Delta E_2 = 8.527$ [J], $K_1^-[\infty] = 21.134$, $K_2^-[\infty] = 19.478$ [J]. Accordingly, we get $K_m^-[\infty] = 20.306$, $\Delta E_m = 9.638$ [J], and $\varepsilon_m = 0.5256$ [-]. Here, we should comment that the value of $K_m^-[\infty]$ is not exactly equal to that of $\Delta E_m/(1-\varepsilon_m)$ because there is a numerical error due to the algorithm in the simulation program for collision detection. We thus use the value obtained from the state variables just before impact instead. This value has satisfactory accuracy for our comparison. In addition, the mean value of the walking speed is $v_m = 0.8074$ [m/s].

We consider discrete-time DFC of a 2-period gait. We formulate the control input based on the half inter-leg angle at impact, α. Note that this α is not the same relative hip-angle as the rimless wheel models, and is defined as

$$\alpha = \frac{\theta_1^- - \theta_2^-}{2} = \frac{\theta_2^+ - \theta_1^+}{2} > 0. \tag{39}$$

The hip-joint torque is formulated as

$$u_2 = \eta\left(\alpha[i] - \alpha[i-1]\right), \tag{40}$$

where $\eta > 0$ is the feedback gain. The robot is then driven by the constant hip-joint torque during stance phases. Fig. 8 shows simulation results of PDW with DFC where $\phi = 0.080$ [rad]. The robot starts from the following initial conditions:

$$\boldsymbol{\theta}(0) = \begin{bmatrix} 0.50 \\ 1.10 \end{bmatrix},\ \dot{\boldsymbol{\theta}}(0) = \begin{bmatrix} 1.10 \\ 0.20 \end{bmatrix}.$$

The optimal feedback gain is found to be $\eta = 0.3155$. The convergent gait, however, returns to the original 2-period gait because the stabilizing control is very weak. In addition, the optimal feedback gait is not easy to find because of the numerical error. We thus should try energy tracking control (ETC) [17] as a means of enhancing stabilization.

Let E^* [J] be the target level of the total mechanical energy. The target condition for ETC can be formulated as

$$\dot{E} = \dot{\boldsymbol{\theta}}^{\rm T}\boldsymbol{S}\boldsymbol{u} = -\lambda\left(E - E^*\right), \tag{41}$$

where $\lambda > 0$ is the feedback gain. The total mechanical energy exponentially converges to its target value, E^*, during stance phases. We will choose E^* to be the value that E converged to in the upper plot of Fig 8. Let $\mu > 0$ be the

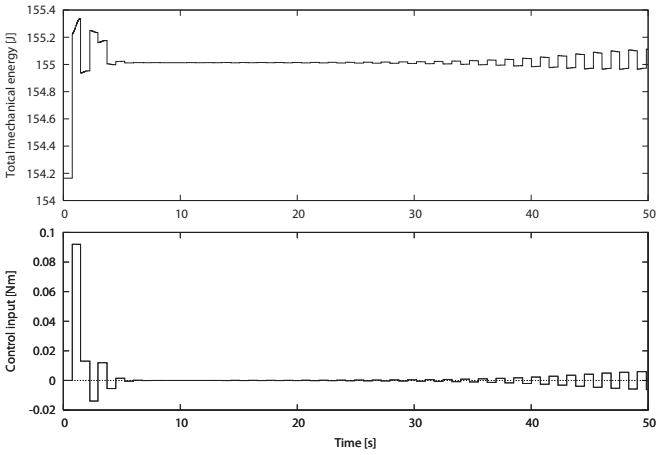

Fig. 8. Simulation results of passive compass-gait with delayed feedback control only. The upper plot is the total mechanical energy, and the lower plot is the control input (hip-joint torque).

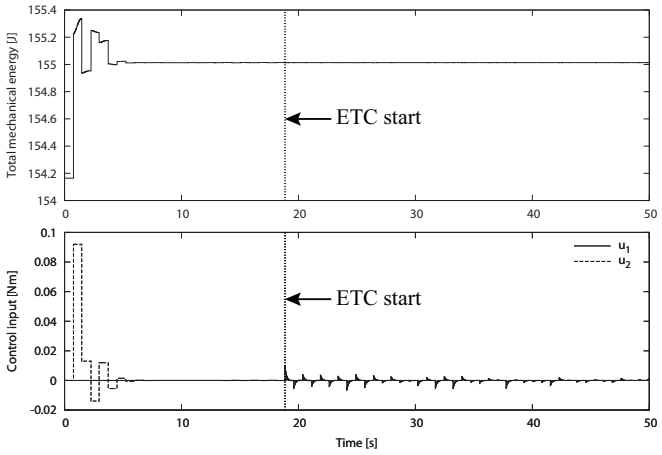

Fig. 9. Simulation results of passive compass-gait with delayed feedback control and energy tracking control. The upper plot is the total mechanical energy, and the lower plot is the control inputs.

constant torque ratio, and substituting the relation $u_1 = \mu u_2$ into Eq. (41), we get

$$\boldsymbol{S}\boldsymbol{u} = \begin{bmatrix} 1 \\ -1 \end{bmatrix} \eta \left(\alpha[i] - \alpha[i-1]\right) + \begin{bmatrix} \mu + 1 \\ -1 \end{bmatrix} \frac{\lambda \left(E^* - E\right)}{(\mu+1)\dot{\theta}_1 - \dot{\theta}_2}. \tag{42}$$

The second term for ETC should vanish like the first term of DFC as the gait converges to an unstable 1-period gait. In this sense, we can consider that the generated 1-period gait is *naturally* stabilized.

Fig. 9 shows simulation results for $E^* = 155.0132$ [J], $\mu = 6.0$, and $\lambda = 10.0$. We can see that the generated gait is a single period and the control inputs are very small. The gait descriptors converge to unique values. The half inter-leg angle converges to $\alpha = 0.3131$ [rad]. Since $\alpha_2 \leq \alpha \leq \alpha_1$ holds, the generated unstable 1-period gait can be considered to be a middle gait. The restored mechanical energy is $\Delta E = 9.661$ [J] and $\Delta E > \Delta E_m$. However, the energy-loss coefficient is $\varepsilon = 0.5241$ [-], and $\varepsilon < \varepsilon_m$; thus the magnitude relation of Eq. (11) does not hold. These results make it difficult to know whether the generated 1-period gait has higher kinetic energy compared with the original 2-period one. There is a possibility that $K^-[\infty] \geq K_m^-[\infty]$ holds because the two magnitude relations are sufficient conditions for it and need not always hold simultaneously. The simulation results give $K^-[\infty] = 20.2974$ [J] and the kinetic energy converges to a value lower than $K_m^-[\infty]$. The walking speed v is, however, 0.8148 [m/s], which is faster than v_m. This result seems contradictory, but it can be understood by the fact that, unlike the case of a rimless wheel, a one-to-one relation between kinetic energy and walking speed does not always hold in dynamic bipedal walking. We must therefore be careful so as not to run away with the idea that the gait efficiency grows worse because the convergent kinetic energy level is lower.

VI. Quasi-constraint on Impact Posture

Swing-leg retraction is a phenomenon that often occurs in limit cycle walking. 'Quasi-constraint on impact posture' is a method to make the robot fall like a 1-d.o.f. rigid body. The authors found that the quasi-constraint dramatically increases limit cycle stability [18]. The velocity condition for a holonomic constraint is given by

$$\dot{\theta}_H = \dot{\theta}_1 - \dot{\theta}_2 = \begin{bmatrix} 1 & -1 \end{bmatrix} \dot{\boldsymbol{\theta}} = \boldsymbol{S}_2^{\mathrm{T}} \dot{\boldsymbol{\theta}} = 0. \tag{43}$$

The holonomic constraint force is given as the following hip-joint torque:

$$u_2 = \left(\boldsymbol{S}_2 \boldsymbol{M}(\boldsymbol{\theta})^{-1} \boldsymbol{S}_2^{\mathrm{T}}\right)^{-1} \boldsymbol{S}_2 \boldsymbol{M}(\boldsymbol{\theta})^{-1} \boldsymbol{h}(\boldsymbol{\theta}, \dot{\boldsymbol{\theta}}). \tag{44}$$

In numerical simulations, the hip-joint torque was switched from 0 to Eq. (44) when $\dot{\theta}_1 = \dot{\theta}_2$. The generated 1-period gait has a holonomic constraint during the stance phase, and the gait property strongly differs from that of the original PDW. In this sense, we should consider that the gait is *unnaturally* stabilized or remade.

Fig. 10 shows the time evolution of angular velocities in steady passive-dynamic gaits with and without a quasi-constraint where $\phi = 0.080$ [rad]. The target stable 2-period gait is the same as in the previous section. From (b), we can see that the quasi-constraint occurs just after $\dot{\theta}_1 = \dot{\theta}_2$, and the generated gait becomes 1-period.

The gait descriptors in the stable 1-period gait with a quasi-constraint converge to $\alpha = 0.3242$ [rad], $\varepsilon = 0.5223$ [-], and $\Delta E = 9.988$ [J]. Since $\alpha_2 \leq \alpha \leq \alpha_1$ holds, the convergent gait can be considered to be a middle gait. In this case, $\varepsilon < \varepsilon_m$ and the magnitude relation of Eq. (11) does not hold, whereas $\Delta E > \Delta E_m$ is satisfied.

In this case, we get $K^-[\infty] = 20.908$ [J] and $K^-[\infty] > K_m^-[\infty]$. This result implies that, when ΔE is sufficiently larger than ΔE_m, the gait efficiency becomes better even if $\varepsilon \leq \varepsilon_m$. Nonetheless, the walking speed converges to $v = 0.7813$ [m/s] and $v < v_m$; i.e. the walking speed is slower than in PDW. This is because a one-to-one relation between kinetic energy and walking speed does not always hold in dynamic bipedal walking.

Table II compares the results of the two stabilizing control effects. From these results, we must conclude that the stabilization to a 1-period gait is not always effective for

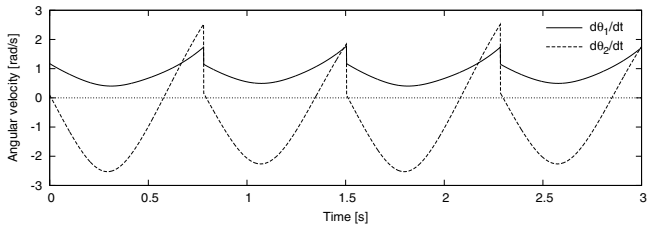

(a)

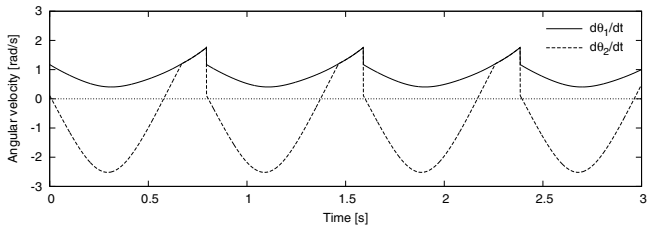

(b)

Fig. 10. Time-evolutions of angular velocities with and without quasi-constraint on impact posture in passive compass-gait where $\phi = 0.080$ [rad]. (a) is the original passive compass-gait without quasi-constraint and is 2-period, and (b) is with quasi-constraint and is 1-period.

TABLE II
RESULTS COMPARISON

Checking item	DFC	Quasi-constraint
$\varepsilon \geq \varepsilon_m$?	No	No
$\Delta E \geq \Delta E_m$?	Yes	Yes
$K^- \geq K_m^-$?	No	Yes
$v \geq v_m$?	Yes	No

improvement of the gait efficiency, and the results cannot be examined without numerical simulations. In this sense, dynamic gaits having two magnitude relations (Eqs. (11) and (13)), which are sufficient conditions for the properties of a rimless wheel, are highly restricted and are not easy to realize. In addition, we must be careful that the kinetic energy is merely an indicator of gait efficiency. The efficiency comparison becomes more complicated when the specific resistance is taken into account.

VII. CONCLUSION AND FUTURE WORK

We discussed the efficiency and optimality of a 2-period gait from the kinetic energy view-point. Numerical simulations of VPDW proved the validity of the method derived from the discrete dynamics of a rimless wheel. Furthermore, the effects of DFC and a quasi-constraint on the impact posture were examined. The results implied that stabilizing a 1-period gait does not always improve gait efficiency and that a gait such as PDW having two magnitude relations is not easy to realize.

In the future, we should theoretically investigate the relation between the convergent kinetic energy level and walking speed in more detail. Although a one-to-one relation between walking speed and kinetic energy holds for a rimless wheel, limit cycle walkers have leg-swing motions that destroys the one-to-one relation. The author considers that the swing-leg retraction is the cause. On the other hand, it is empirically known that the hip damper extends the stable domain [8] and eliminates chaotic behavior in passive gaits [19]. An investigation of the hip damper effect on gait efficiency would also be an interesting subject. Extension of our approach to general multiple-period cases, i.e., 2^n-period and chaotic gaits, should also be investigated.

REFERENCES

[1] T. McGeer: "Passive dynamic walking," *Int. J. of Robotics Research*, Vol. 9, No. 2, pp. 62–82, 1990.
[2] F. Asano, Z.W. Luo and M. Yamakita: "Biped gait generation and control based on a unified property of passive dynamic walking," *IEEE Trans. on Robotics*, Vol. 21, No. 4, pp. 754–762, 2005.
[3] F. Asano and Z.W. Luo: "Energy-efficient and high-speed dynamic biped locomotion based on principle of parametric excitation," *IEEE Trans. on Robotics*, Vol. 24, No. 6, pp. 754–762, 2008.
[4] A. Goswami, B. Thuilot and B. Espiau: "Compass-like biped robot part I: Stability and bifurcation of passive gaits," *Research report, INRIA*, No. 2996, 1996.
[5] M. Garcia, A. Chatterjee and A. Ruina: "Speed, efficiency, and stability of small-slope 2D passive dynamic bipedal walking," *Proc. of the IEEE Int. Conf. on Robotics and Automation*, Vol. 3, pp. 2351–2356, 1998.
[6] M. Garcia, A. Chatterjee, A. Ruina and M. Coleman: "The simplest walking model: Stability, complexity, and scaling," *ASME J. of Biomechanical Engineering*, Vol. 120, No. 2, pp. 281–288, 1998.
[7] M. Garcia, A. Chatterjee and A. Ruina: "Efficiency, speed, and scaling of two-dimensional passive-dynamic walking," *Dynamics and Stability of Systems*, Vol. 15, No. 2, pp. 75–99, 2000.
[8] A. Goswami, B. Thuilot and B. Espiau: "A study of the passive gait of a compass-like biped robot: Symmetry and chaos," *Int. J. of Robotics Research*, Vol. 17, No. 12, pp. 1282–1301, 1998.
[9] A. Sano, Y. Ikemata and H. Fujimoto: "Analysis of dynamics of passive walking from storage energy and supply rate," *Proc. of the IEEE Int. Conf. on Robotics and Automation*, Vol. 2, pp. 2478–2483, 2003.
[10] K. Osuka and K. Kirihara, "Motion analysis and experiments of passive walking robot Quartet II," *Proc. of the IEEE Int. Conf. on Robotics and Automation*, Vol. 3, pp. 3052–3056, 2000.
[11] E. Ott, C. Grebogi and J. A. Yorke, "Controlling chaos," *Physical Review Letters*, Vol. 64, No. 11, pp. 1196–1199, 1990.
[12] K. Pyragas, "Continuous control of chaos by self-controlling feedback," *Physics Letters A*, Vol. 170, No. 6, pp. 421–428, 1992.
[13] Y. Sugimoto and K. Osuka, "Walking control of quasi-passive-dynamic-walking robot 'Quartet III' based on delayed feedback control," *Proc. of the 5th Int. Conf. on Climbing and Walking Robots*, pp. 123–130, 2002.
[14] S. Suzuki and K. Furuta: "Enhancement of stabilization for passive walking by chaos control approach," *Proc. of the 15th Triennial World Congress of the International Federation of Automatic Control*, 2002.
[15] F. Asano and Z.W. Luo: "Pseudo virtual passive dynamic walking and effect of upper body as counterweight," *Proc. of the IEEE/RSJ Int. Conf. on Intelligent Robots and Systems*, pp. 2934–2939, 2008.
[16] F. Asano and Z.W. Luo, "Asymptotically stable biped gait generation based on stability principle of rimless wheel," *Robotica*, 2009. (In press)
[17] A. Goswami, B. Espiau and A. Keramane, "Limit cycles in a passive compass gait biped and passivity-mimicking control laws," *Autonomous Robots*, Vol. 4, No. 3, pp. 273–286, 1997.
[18] F. Asano and Z.W. Luo, "Robust pseudo virtual passive dynamic walking considering swing-leg retraction," *Proc. of the 26th Annual Conf. of the Robotics Society of Japan*, 3B1-05, 2009. (In Japanese)
[19] M. J. Kurz and N. Stergiou, "Hip actuations can be used to control bifurcations and chaos in a passive dynamic walking model," *J. of Biomechanical Engineering*, Vol. 129, No. 2, pp. 216–222, 2007.